

PRELIMINARY SHOCK PRESSURE CALIBRATION CURVE FOR EXPERIMENTALLY SHOCKED BYTOWNITE.

Y. Li^{1,2}, F. Cao^{1,2}, T.W. Matterson¹, R.L. Flemming^{1,2}, S.J. Jaret³, J.R. Johnson⁴, P.J.A. McCausland^{1,2} ¹Department of Earth Sciences and ²Institute for Earth and Space Exploration, Western University, London, ON, Canada N6A 5B7 ³Department of Earth and Planetary Sciences, American Museum of Natural History, New York, NY, USA, ⁴Johns Hopkins University Applied Physics Laboratory, Laurel, MD, USA.

Introduction: Shock metamorphism results from hypervelocity impact between objects with an extreme deformation strain rate ($>10^6/\text{s}$) [1-2]. Rapid volume compression and decompression of the shocked body creates a large amount of strain energy in the crystal structure, and it has been described as the destructive effect of shock deformation [2]. Petrographically, it is observed as increasing subdomain misorientation of shocked crystals (e.g. plagioclase, olivine) showing textures such as undulatory extinction, mosaicism, and recrystallization, from low shock to high shock. Other textures such as fractures, planar fractures, or planar deformation features are also sometimes observed in shocked crystals. Petrographic observation of textures has been used to determine the shock stage in meteorites [e.g., 2-4].

For polished sections, two-dimensional (2D) X-ray diffraction (XRD) of in situ crystal locations produces structurally related diffraction spots along the 2-theta and chi dimensions, and it has been observed that non-uniformly strained crystals display a mosaic spread of diffraction spots along the Debye ring or chi direction. On 2D XRD images, line shape changes from discrete single spots (non-shocked) to streaks (shocked). In some cases, it will show a row of spots diffracted from large subdomains in the shocked crystal, called asterism [5-7]. Collectively, streaking and asterism in 2D XRD observations of deformed crystals are called strain-related mosaicism (SRM) [5-15]. Quantitative SRM analysis measures full width at half maximum (FWHM) of the peak profile integrated from 2D XRD patterns along the chi direction (χ), in which it has been observed that $\text{FWHM}\chi$ increases with increasing shock degree [8-15]. The method has been further developed by using an empirical peak fitting program coded in Matlab®, Best Fit for Complex Peaks (BFCP), to measure asymmetrical peaks integrated from complex SRM patterns in highly strained crystals, reported as $\Sigma(\text{FWHM}\chi)$ [10-11]. Both $\text{FWHM}\chi$ and/or $\Sigma(\text{FWHM}\chi)$ have been used to quantitatively describe the shock degree in minerals in various meteorites such as enstatite in enstatite chondrites, plagioclase in lunar meteorites, and olivine in martian meteorites, ordinary chondrites and ureilites [8-14].

To put the empirical SRM methods on a more quantitative footing, reference to experimentally shocked samples is needed. Quantitative SRM analysis is used on experimentally shocked samples and we observe a linear trend for $\text{FWHM}\chi$ and $\Sigma(\text{FWHM}\chi)$ as a function of experimental shock pressure. For natural unknowns, the peak shock pressure can be directly measured from the calibration curve by giving the measured $\text{FWHM}\chi$

or $\Sigma(\text{FWHM}\chi)$ of the investigated mineral in shocked meteorites. This method has been tested on andesine plagioclase in a martian regolith breccia meteorite [15]. In this work, we used experimentally shocked Ca-rich bytownite plagioclase [16] to develop a preliminary SRM calibration curve for shocked bytownite. We have measured quantitative SRM as both $\text{FWHM}\chi$ and $\Sigma(\text{FWHM}\chi)$ (using Best Fit for Complex Peaks [10]).

Method: Bytownite samples used in this study are Ca-rich plagioclase (An₇₇) that were shocked experimentally to pressures between 17 to 56.3 GPa. The measurements were performed on thin sections of fragments of materials extracted during the original shock experiments, and more detail about experiments can be found in previous publications [16-19]. Five experimentally shocked bytownite were selected to generate the calibration curves, and they were shocked to pressures of 17.0, 22.6, 29.3, 38.2, and 56.3 GPa, respectively. One unshocked bytownite with pressure 0 GPa was also studied in this work. X-ray diffraction data were collected using a Bruker D8 Discover μXRD at Western with a Co K α X-ray source (λ Co K α_1 = 1.78897 Å; nominal beam diameter = 300 μm) and Vantec-500 detector, with General Area Detector Diffraction System (GADDS) software [5], obtaining 2D diffraction patterns similar to Debye-Scherrer film. SRM analysis was performed by Bruker DiffracPLUS EVA® (all samples) and BFCP [10]. For BFCP, a Pseudo-Voigt function is used to generate an empirical peak fitting model to fit the peak profile and measure $\Sigma(\text{FWHM}\chi)$. We compare two calibration curves below, using simple peak measurements, $\text{FWHM}\chi$, and summation measurements, $\Sigma(\text{FWHM}\chi)$, fitted by BFCP. Preliminary $\Sigma(\text{FWHM}\chi)$ curve used four shocked samples (22.6 GPa is not measured for now due to time constraints).

Results: The shocked samples show a mosaic spread along the chi dimension indicating the misorientation of the subdomains in the shocked bytownite crystals (Fig.1). As shock pressure increases from 0 GPa to 56.3 GPa, the overall diffraction intensity of 2D XRD images decreases, and a trend of increase in streak length with respect to increase of shock pressure is observed. $\Sigma(\text{FWHM}\chi)$ and $\text{FWHM}\chi$ results are summarized in Table 1. Five samples yield the linear trendline of $\Sigma(\text{FWHM}\chi)$ as the function of experimentally shocked pressure $\Sigma(\text{FWHM}\chi) = 0.33 * \text{Pressure} + 0.92$ with R^2 of 0.9741 indicating a good linear fit (Fig. 2A). Simple peak calibration curve with six samples yields the function of $\text{FWHM}\chi = 0.10 * \text{Pressure} + 0.96$ with R^2 of 0.9803 indicating a good linear fit (Fig. 2B). The

intersection values at y-axis when shock pressure is 0 GPa are similar in both calibration curves. The increased slope value in the calibration curve by $\Sigma(\text{FWHM}\chi)$ is due to the larger measurements from BFCP. BFCP provided empirical peak fitting when handling the non-uniform peak distribution profile (e.g., Fig. 1D, F, H, L), and it measured the sum of $\text{FWHM}\chi$ from fitted peaks, resulting in the larger value compared to treating the data as simple peaks (Fig. 1F & 1L).

Table 1. $\Sigma(\text{FWHM}\chi)$ and $\text{FWHM}\chi$ fit statistics for bytownite.

Pressure	Methods	Ave.	STDEV	N
0.0 GPa	$\Sigma(\text{FWHM}\chi)$	1.42	0.49	7
(unshocked)	$\text{FWHM}\chi$	0.83	0.39	46
17.0 GPa	$\Sigma(\text{FWHM}\chi)$	6.58	1.70	9
(3156)	$\text{FWHM}\chi$	3.08	1.10	41
22.6 GPa	$\Sigma(\text{FWHM}\chi)$	n/a	n/a	n/a
(3155)	$\text{FWHM}\chi$	3.22	1.47	41
29.3 GPa	$\Sigma(\text{FWHM}\chi)$	8.90	1.48	4
(3142)	$\text{FWHM}\chi$	4.12	1.17	34
38.2 GPa	$\Sigma(\text{FWHM}\chi)$	15.05	6.35	5
(3143)	$\text{FWHM}\chi$	4.46	3.01	20
56.3 GPa	$\Sigma(\text{FWHM}\chi)$	19.90	2.81	3
(3144)	$\text{FWHM}\chi$	6.93	3.62	20

Note: Ave. = average. STDEV = standard deviation. N = number of data used for calculating the average at each pressure. Run # appears below pressure. More data, including 22.6 GPa, will be processed using BFCP ($\Sigma(\text{FWHM}\chi)$) in future.

Future work: Further work will analyze more data to include in the preliminary calibration curve by both methods. We will also compare with different plagioclase composition calibration curves [e.g., 15] to assess the effect of feldspar composition on shock damage [16], and the use of plagioclase calibration curves in tandem with those developed for other ubiquitous rock-forming minerals: olivine [9, 11, 14] and pyroxene [13] for quantitative SRM analysis of natural samples.

Reference: [1] French (1998) Technical Report, LPI-Contrib-954. [2] Fritz et al., (2017) MAPS, 52, 1216–1232. [3] Stöffler et al. (1991) GCA, 55, 3845–3867 [4] Stöffler et al. (2018) MAPS, 53, 5–49. [5] Flemming (2007) CJES, 44, 1333–1346. [6] Hörz and Quaide (1973) The Moon, 6, 45–82. [7] Vinet et al. (2011) Am Min., 96, 486–497. [8] Pickersgill et al. (2015) MAPS, 50, 1851–1862. [9] Jenkins et al. (2019) MAPS, 54, 902–918. [10] Li et al. (2020) C&G, 144, 104572. [11] Li et al. (2021), MAPS, 56, 1422–1439. [12] McCausland et al. (2010) AGU Abs. # P14C-031. [13] Izawa et al. (2011) MAPS, 46, 638–651. [14] Rupert et al. (2020) MAPS, 55(10), 2224–2240. [15] Cao et al. (2020) LPSC Abs. # 2326, p. 2114 [16] Jaret, S. J., et al. (2018) JGR: Planets, 123(7), 1701–1722. [17] Johnson et al. (2002) JGR, 107(E10), 5073. [18] Johnson et al. (2003) Am Min., 88(10), 1575–1582. [19] Johnson (2012) Icarus, 221(1), 359–364.

Acknowledgement: RLF and PJAM acknowledge research funding support from NSERC – Discovery Grants. TWM acknowledges Western USRI funding.

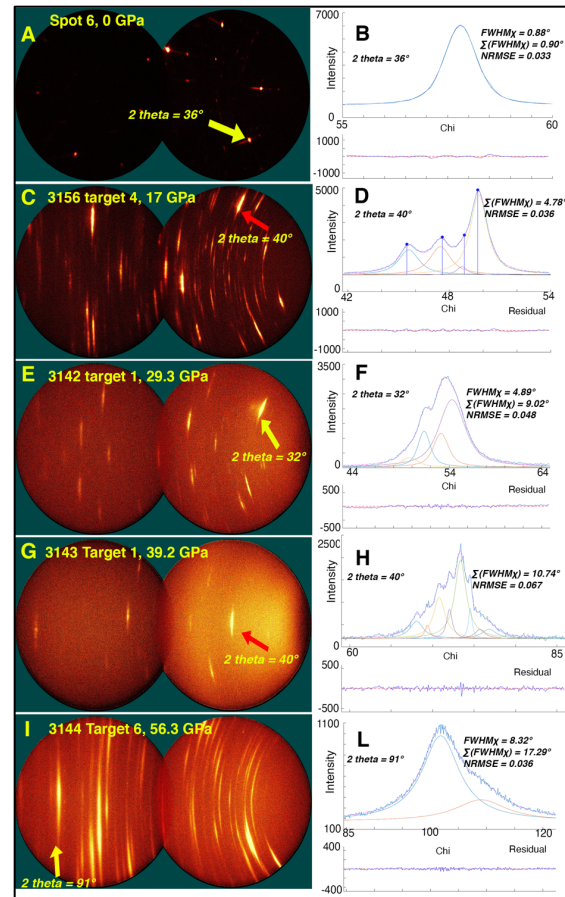


Fig. 1. Representative XRD images and e.g. peak fits for bytownite. $\Sigma(\text{FWHM}\chi)$ for the integrated peak profile increases from shock pressure 0 GPa to 56.3 GPa (1A to 1L).

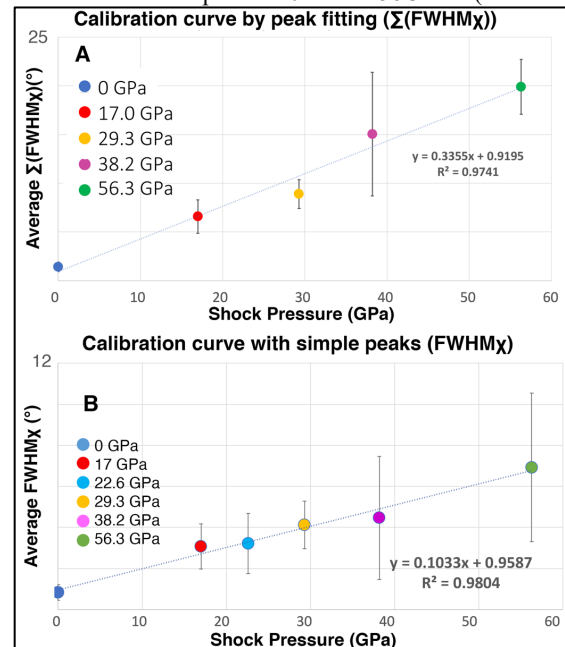


Fig. 2. Preliminary bytownite calibration curves. 2A from peak fitting. A total five samples are used in the curve. 2B is from simple peak measurements with six samples in total.